LABORATORY BASED PHYSICAL INVESTIGATION OF RAINFALL INDUCED LANDSLIDE WITH SOIL MOISTURE CONTENT MEASUREMENTS

A

THESIS

Submitted in partial fulfillment of the requirements for the award of the degree of

MASTER OF TECHNOLOGY
IN
CIVIL ENGINEERING

With specialization in

STRUCTURAL ENGINEERING

Under the supervision of

Dr. Ashok Kumar Gupta (Dean – Academics & Research)

Mr. Chandra Pal Gautam (Assistant Professor)

by

Ananay Sambyal (212651)

to

JAYPEE UNIVERSITY OF INFORMATION TECHNOLOGY

WAKNAGHAT, SOLAN – 173234

HIMACHAL PRADESH, INDIA

May 2023

STUDENT'S DECLARATION

I hereby declare that the work presented in the Project report entitled **"LABORATORY BASED PHYSICAL INVESTIGATION OF RAINFALL INDUCED LANDSLIDE WITH SOIL MOISTURE CONTENT MEASUREMENTS"** submitted for partial fulfillment of the requirements for the degree of Bachelor of Technology in Civil Engineering at **Jaypee University of Information Technology, Waknaghat** is an authentic record of my work carried out under the supervision of **Dr. Ashok Kumar Gupta** and **Mr. Chandra Pal Gautam**. This work has not been submitted elsewhere for the reward of any other degree/diploma. I am fully responsible for the contents of my project report.

Signature of Student
Name: Ananay Sambyal
Roll No: 212651
Department of Civil Engineering
Jaypee University of Information Technology, Waknaghat
Date:

CERTIFICATE

This is to certify that the work which is being presented in the project report titled **"LABORATORY BASED PHYSICAL INVESTIGATION OF RAINFALL INDUCED LANDSLIDE WITH SOIL MOISTURE CONTENT MEASUREMENTS"** in partial fulfillment of the requirements for the award of the degree of Master of Technology in Civil Engineering submitted to the Department of Civil Engineering, Jaypee University of Information Technology, Waknaghat is an authentic record of work carried out by **Ananay Sambyal (212651)** during the period from July, 2022 to May, 2023 under the supervision of **Dr. Ashok Kumar Gupta** and **Mr. Chandra Pal Gautam**, Department of Civil Engineering, Jaypee University of Information Technology, Waknaghat.

The above statement made is correct to the best of our knowledge.

Date:

Signature of Guide
Dr. Ashok Kumar Gupta
Dean – Academics & Research
JUIT Waknaghat

Signature of HOD
Dr. Ashish Kumar
Department of Civil Engineering
JUIT Waknaghat

Signature of Co-Guide
Mr. Chandra Pal Gautam
Assistant Professor (Grade II)
Department of Civil Engineering
JUIT Waknaghat

ACKNOWLWDGEMENT

First and foremost, I would like to praise and thank God, the almighty, for blessing me with countless opportunities, knowledge and giving me strength, energy and patience to overcome all the difficulties to reach this ambition.

I would like to express the deepest appreciation for my guide, Mr. Ashok Kumar Gupta, for his continual supervision and valuable feedback. He has provided me with insightful comments on my research that have been a substantial aid in this accomplishment. Without his guidance and persistent support, I would never have been able to complete my dissertation. I sincerely express my deep sense of gratitude to my co-guide Mr. Chandra Pal Gautam for his untiringly support and sincere guidance.

I am indebted to Dr. Surabh Rawat and Dr. Tanmay Gupta for their concern, scientific motivation, encouragement and for providing all necessary knowledge in completing this project. I thank them from the bottom of my heart.

I also acknowledge support and cooperation provided by all the lab staff and non-teaching staff members of Department of Civil Engineering.

Most of all, this dissertation is dedicated to my beloved family, especially my mother. This acknowledgment would not be complete without mentioning their pain staking efforts and patience. No words are adequate to express my indebtedness to my parents and my younger brother for their support. I owe this thesis to them. This achievement of my life would not be possible without their support and cooperation throughout this study.

Lastly, I express my hearty thanks to those whom I might have missed to mention by name, who helped me directly or indirectly and co-operated with me a lot in completion of this research work.

Ananay Sambyal

ABSTRACT

Countless lives are lost every year throughout the world due to slope failures. This problem is more prevalent in mountainous areas. Invaluable lives could be saved if proper warning is given beforehand. Researches all around the world are being done so that systems could be developed that can forecast the disaster before it inflicts damage. Technological advancements have led to close the gap for this feat. But there is still time, before its preciseness could be close to inch-perfect and the technology becomes accessible for every community. The biggest problem lies with vastness in nature and properties of soil slopes. Different slopes react differently to instability caused by various triggering factors such as rainfall or ground shaking. To tackle it, thorough investigation on various slopes is done by engineers and researchers from various fields. Proper understanding of failure mechanisms and knowledge of engineering properties of soil is must. It is just a matter of time, before proper landslide forecasting technology develops which is as accepted as weather forecasting.

In my project, I have predominantly focused on lab testing on two flume models made from locally available soil. Both slope models have been made at different angles of 60° and 70°. Instability was created from simulated rainfall and intensity of rain was kept same for both models. Soil moisture content readings were also taken using small sensors. The failure mechanism and features have been expounded upon. Toe area of a slope has been found of great importance as per sensor readings, which has been discussed in this dissertation.

A cantilever retaining wall has also been designed for an in situ slope. It was verified using Geo5 software, where it passed all the checks. The stability analysis of the chosen slope has been done before and after the construction of retaining wall on it, to determine its Factor of Safety. A substantial increment the FOS was observed.

There is still scope for further research with improved models and instruments.

Keywords: Retaining wall, Slope stability, Moisture content, Tension crack, Overturning

TABLE OF CONTENTS

LIST OF TABLES

LIST OF FIGURES

LIST OF ACRONYMS

UNSC	Unified Soil Classified System
GPS	Global Positioning system
RST	Remote Sensing Techniques
OMC	Optimum Moisture Content
VMC	Volumetric Moisture Content
NH	National Highway
FOS	Factor of safety
CG	Centre of Gravity
SBC	Soil Bearing Capacity
BM	Bending Moment
SF	Shear Force
MCU	Micro Controller Unit
IoT	Internet of Things
TSMC	Taiwan Semiconductor Manufacturing Company
GL	Ground Level

CHAPTER 1

INTRODUCTION

1.1 General

Landslides are among the world's most potent geo hazards, threatening both citified and countryside areas. Every year, these disasters cost incalculable number of human lives and create enormous economic losses in various regions of the world. Landslides have also contributed to long-term environmental devastation. Rainfall is a major cause of soil slope failure throughout the world. As a result of climate change, the frequency and intensity of rainfall has increased, as well as its pattern has changed, which considerably raises the danger of landslides in landslide-prone areas. Rainfall-induced soil slope failures (landslides) have been observed during or soon after periods of extreme or protracted heavy rain. These soil collapses can occur on both natural and man-made slopes. It is also seen in the field that cut slopes and slope embankments are susceptible to these type of failures. Due of the severity of the landslide danger, many scientists and engineers are working to advance landslide research and lower the risk of landslides. Because rainfall is so closely related to landslides, scientists have been working to create effective techniques for forecasting landslides based on rainfall features and soil response. Improved understanding of internal response of soil in the process of rainfall-induced landslides is essential for better landslide prediction. Field measurements and laboratory testing have typically contributed to a better understanding of the mechanics and circumstances that lead to the onset of these failures. For many years, landslide modelling relied only on numerical modelling approaches. Modelling of landslides using physical scaled models of landslides first started in Japan in 1970s on natural slopes subjected to fabricated rainfall [1-4]. Large-scale debris flow tests were carried out in the United States in 1990s [5,6]. Laboratory testing under unit acceleration conditions in scaled down physical models (also known as flume tests) began in 1980s and 1990s in Japan [3], Canada [7] and Australia [8]. Landslide modelling on a small scale has found widespread application in analyzing various types of landslides (e.g., flows, slides, falls, topples, etc.) in various materials (sandy, silty, clayey, etc.) and with varying boundary conditions, as well as the ability to analyze a broad range of mechanisms and processes.

1.2 What is a landslide?

The study of Landslide can be discrete. Different professionals such as engineers, geologists, etc. frequently define landslides in a moderately distinctive way. This diverseness in reference depicts the complexity in essence of the numerous professions that are associated in studying the phenomena of landslide. The term landslide describes the movement of a mass of rock, debris or earth downslope [9]. Figure 1.1 shows the geometry of a landslide (Cornforth, fig. 1.1, p. 4) [10].

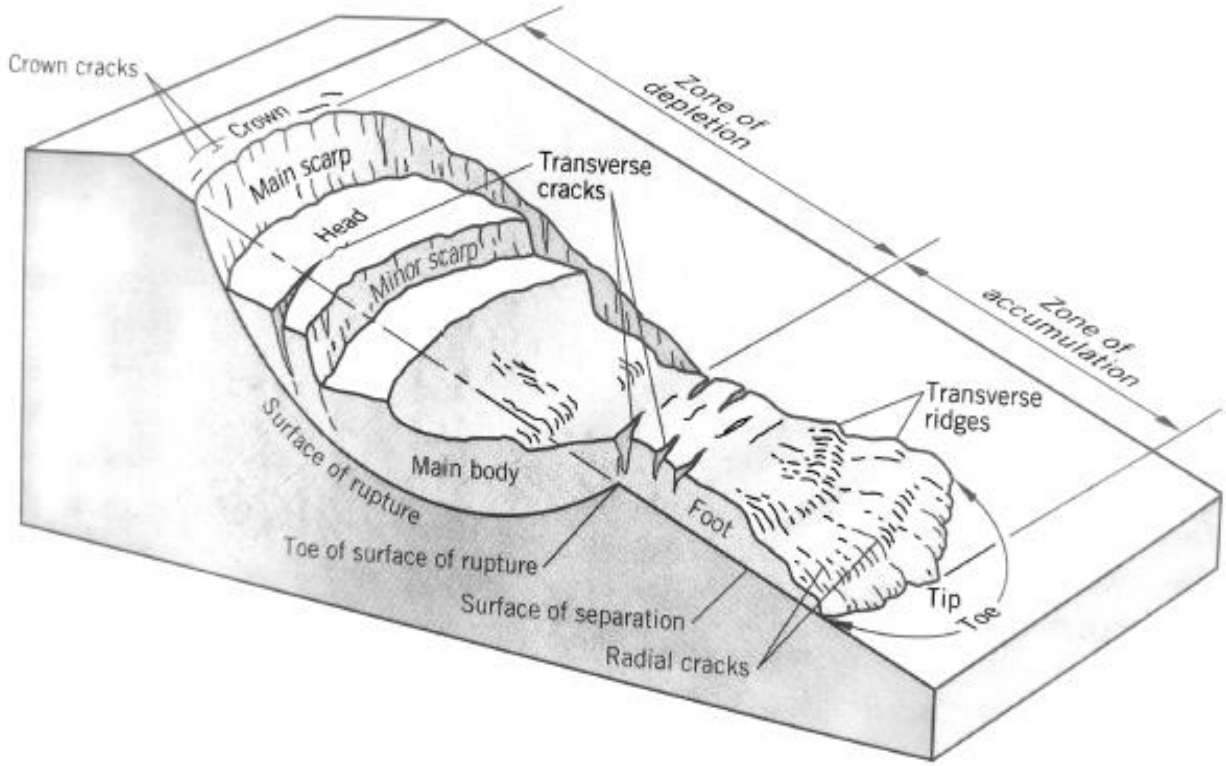

Figure 1.1 Geometry of a landslide

These components of a landslide are described as follows [10]-

1. Crown- The material that is practically undisplaced and is located adjacent to the highest part of the main scarp.
2. Main scarp- Steep surface on the ground that is undisturbed, located at the upper edge of the landslide.
3. Minor scarp- Steep surface on displaced material which is produced by differential shifts within displaced material.

4. Surface of rupture- Surface which forms the lower boundary of displaced material below primary ground surface.
5. Toe of surface of rupture- Convergence between primary ground surface and lower part of surface of rupture.
6. Head- Upper part of the landslide with contact between the main scarp and displaced material.
7. Foot- Chunk of landslide that has displaced beyond toe of surface of rupture.
8. Toe- The most distinct, usually curved margin of the displaced material, from main scarp.
9. Main body- Part of displaced material which overlies the surface between the toe of surface of rupture and main scarp.
10. Flank- Material that is undisplaced and lies adjacent to the sides of surface of rupture.

1.3 Categorization of landslides

The slope movements have been divided into six categories as per the initial work by Varnes [11] and partly revised by Cruden and Varnes [12]. These divisions are as follows-

1. Falls
2. Topples
3. Slides – rotational and translation
4. Lateral Spreads
5. Flows
6. Composites – Amalgamation of varieties

Figure 1.2 shows examples of landslide occurrences (Cornforth, fig 1.3, p. 6) [10].

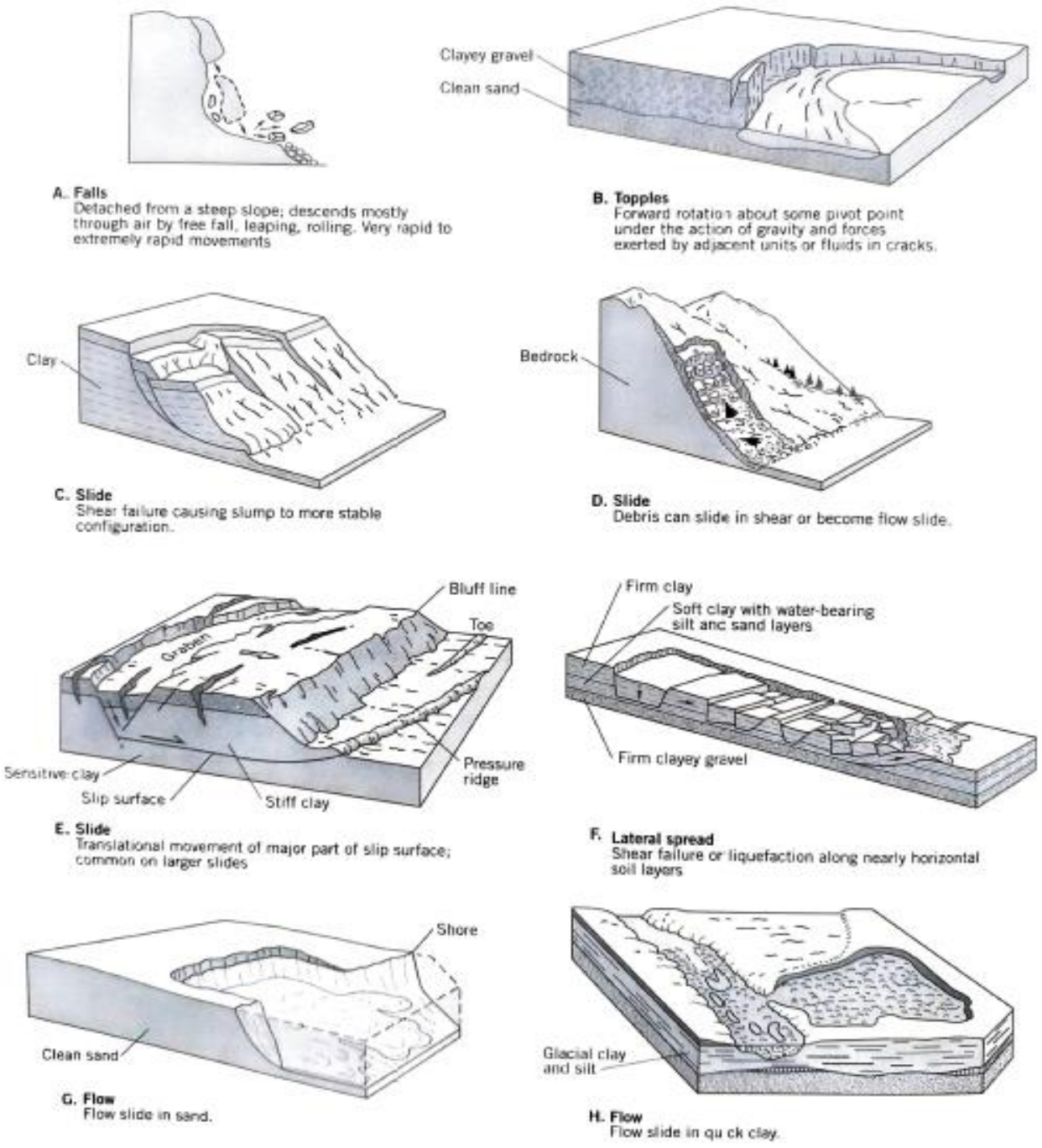

Figure 1.2 Examples of landslide occurrences

1.4 Mechanism of a landslide

Some fundamental laws help us to understand various physical processes going on in our surroundings. These laws also provide us with a more logical way of understanding the mechanism behind the occurrence of a landslide. Let us apply some of these laws to understand the mechanism of a landslide [13].

- According to the "Law of Conservation of Mass" (in relation to the phenomena of Landslide), "The total mass of the reactant (slope), must be equal to the mass of the product". This reaction is supported by several other factors such as rainfall, seismic activity, etc., which act as a catalyst and results in the release of a lot of energy. As a lot of energy is liberated, the nature of this reaction is exothermic. Mass movement of soil or rock mass has a mammoth energy signature, therefore resulting in a lot of destruction of objects in its path. The enormity of destruction depends on how much energy is released.

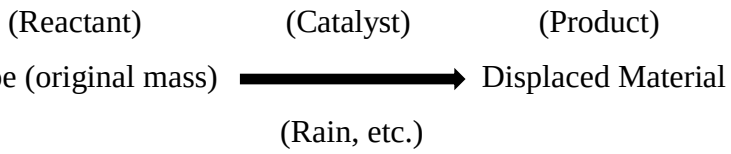

- According to the "Equation of Relativity", "The energy that is released with mass movement of soil or rock mass, is equal to the product of displaced material and velocity of displacement squared".

  E = mc^2

  where,

  E = Energy

  M = Mass of displaced material

  C = velocity of displacement

  The amount of energy released is dependent upon the quantity of the material that is being displaced and the velocity of that material downslope.

- According to the "Law of Gravitational Force of Attraction", "The resistance force is directly proportional to the force of gravity and total mass of material that will displace in case of a landslide".

$$F = \frac{g*M1*M2}{\alpha}$$

where,

g = gravity

M1 = mass of slope

M2 = mass of objects that overly slope (e.g. trees, houses, etc.)

α = inclination of slope

When LHS will be less than RHS, landslide will occur.

- We can also apply the concept of "Limiting Equilibrium" for our perception of mechanism of landslide. "When the forces that induce ground movement are greater than the forces that resist it, landslide will occur". The synergy between the gravity and the resistance to motion plays a crucial role for slope stability. The diminution of the latter will lead to a landslide.

1.4.1 Causes of landslides

There are primarily two aspects that contribute to the occurrence of landslides. Natural reasons and Human infliction. Sometimes they occur or are made worse by the merger of these two factors.

Natural Causes

This category consists of three major triggering factors, which are described below.

- Water

The main cause of landslide is due to soil saturation. One of the primary reasons of slope collapse due to rainfall is a decrease in shear strength as the water content of unsaturated soil increases [14]. Saturation of slope can occur due to various reasons such as, heavy rainfall, snow melting, ground water level changes along earth dams, coast lines, streams, etc. Flooding is also closely related with landslides. Water flowing in streams can penetrate or undercut the banks, which can saturate the slopes, which may cause landslides. In inverse, flooding can also be caused by landslides. Solid landslide debris can block the otherwise flowing streams, which can cause flood like situation at the upstream end of blockage. In real life situations, the biggest cause of landslides triggered by water is due to heavy rainfall. Heavy rainfall tends to degrade the stability of slopes and this risk is further amplified if the slope is at steep angles.

- Seismic Activities

Numerous mountainous areas have experienced landslides due to earthquake activity. Mountains that are prone to landslides because of their geological composition, have a reasonable high chance of landslides because of shaking of ground. The ground shaking cause liquefaction of certain prone sediments or dilate soil mass which can result in manifestation of earth movement downslope. The Kangra earthquake (1905), with magnitude of 7.8, caused many landslides around the region which resulted in tons of landslide related deaths [15]. This tells us how devastating can earthquake be when it comes to triggering landslides.

- Volcanic Activities

Slope movement as a result of volcanic activity constitute some of the most catastrophic failures. Snow can be melted rapidly by volcanic lava, which can form a deluge of rocks, soil and ash that advances rapidly on the abrupt slopes of volcanoes, destroying everything in its path. This volcanic mass may flow to very long distances from their original source. Anything that comes in the path of its flow can sustain damage. When this flow will solidify, it will create a weak geological mass. This weak mass can further fail anytime giving rise to landslides in their surrounding areas. Also the mass can hinder the flow of any stream and can cause havoc in that area.

Human Activities

The rapid increase in population is a severe problem for several countries and overall a major cause of concern for the world. The amount of land and resources stay the same but the population is increasing. To satisfy the needs of this growing population, new settlements are established and developmental activities are continuously being undertaken. New building, dams, highways, canals, etc. are built on regular basis for catering the needs of overgrowing population. The population expand in already created colonies and also move onto new lands. By doing this, humans contribute to more frequent occurrences of landslides. The slopes are destabilized, drainage patterns are changed, and the vegetation is removed during construction activities. These factors can single handedly or by adding up with other factors can cause landslides in the areas prone to it. However, the risk of landslides in these prone areas can be significantly decreased if the developmental activities are carefully engineered.

1.5 Remedial and preventive measures

There are several methods for the stabilization of slopes so that failures can be prevented. Each method is different to other with respect to the method of construction, design perspective, cost of construction, type of slope on which it is to be applied, etc. Also some methods are suitable only for larger landslides and some only for smaller ones. As the technology is evolving, newer techniques are being developed and the current ones are being improved. Some of the options for prevention of landslides or slope stabilization are discussed below briefly [10].

- Dewatering systems

The effective stress acting on the soil affects its strength, therefore if the pore water pressures are decreased on the slip surface of the soil, the stability of the soil can be increased. This method is commonly adopted when the interference is made to geological conditions by humans with native regime of groundwater. There are many ways of dewatering the slope like, through horizontal drains, trench drains, drain blankets, ejector systems, etc. But the outcome of dewatering has mixed success. Because the lateral discontinuity is the nature of many landslides, therefore it can be difficult to make contact with permeable strata by the proposed method of dewatering. Also if there is a lack of permeable ground, then it can become difficult to dewater or depressurize the slope. Thorough investigation is done by geotechnical engineers before they make a call to go with this method.

- Seepage Barriers

When a permeable stratum is underlain by an impermeable stratum, the water from the perimeters of a surrounding entity, such as a river, canal reservoir, etc., can seep out and reach into permeable stratum. In such cases the ground water level in the permeable soil can increase, thereby destabilizing the slope downstream. Seepage barriers can be installed in such cases. Permeability in sub surface is checked using in-situ tests to determine the length and depth that is required for a seepage barrier. Figure 1.3 helps to visualize this concept (Cornforth, fig.18.1, p. 363) [10].

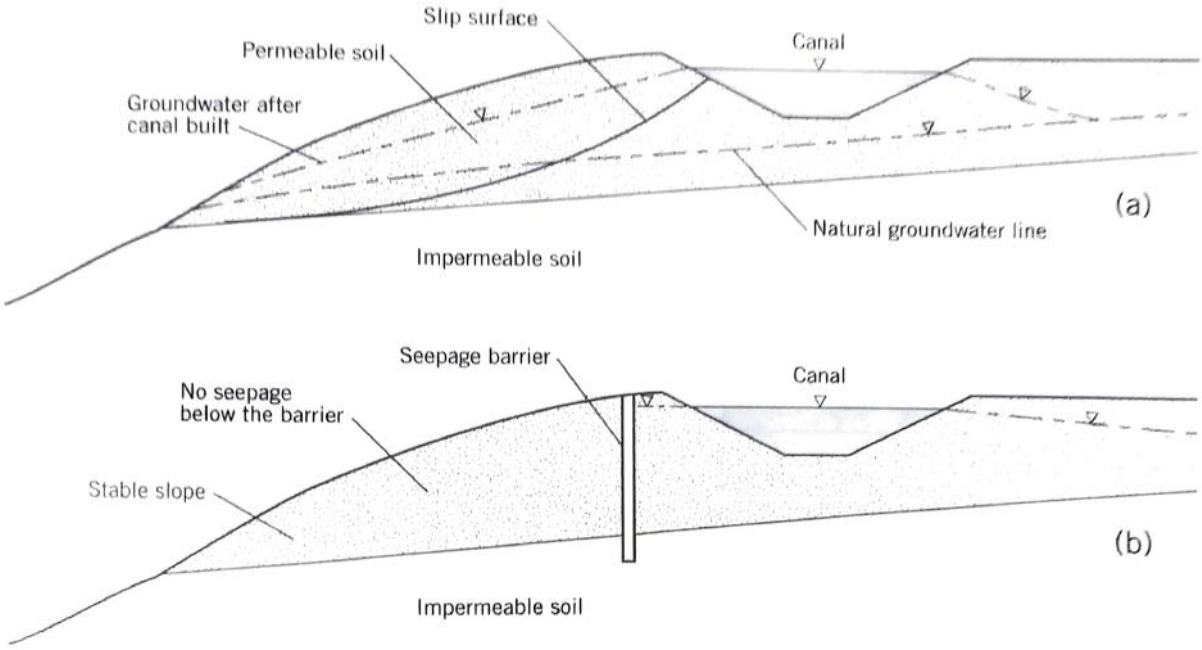

Figure 1.3 Seepage barrier

- Retaining Walls

Retaining wall is another effective remedy for slope failure, in which relatively stiff walls are used to support the mass of soil laterally and the level of soil on two sides is different. The design of retaining walls is complex and depends on factors such as earth pressures, shear forces, bending moments, etc. An experienced engineer can very well do this task. Retaining walls can be broadly classified into four categories [10].

1. Gravity walls (wall foundation provides resistance to sliding and overturning)
2. Cantilever walls (vertical or inclined cantilever provides support)
3. Tie Back walls (outward deflection is restricted by ground anchors on face of wall)
4. Reinforced soil walls (metal strips, grids etc. reinforces soil to allow outer face of wall to stand at comparatively steep slopes)

- Reinforcement of Earth

In this method various tension resisting materials are tucked inside the slope to make it more stable. Steel rods, metal strips, grids, cloth geo synthetics, steel angles, etc. are these tension resisting materials. These materials are relatively cheaper than conventional retaining walls. Also they possess certain other advantages such as flexibility, ease of construction, etc. As a

result of these benefits their use has increased rapidly. There are various techniques of reinforcing the earth by these materials such as- Soil nailing (to improve stability, parallel steel bars are installed spaced closely), Micropiling (bored piles of small diameter in which steel reinforcement is grouted), etc. The figure below shows various types of soil reinforcement material (Cornforth, fig.20.24, p. 444) [10].

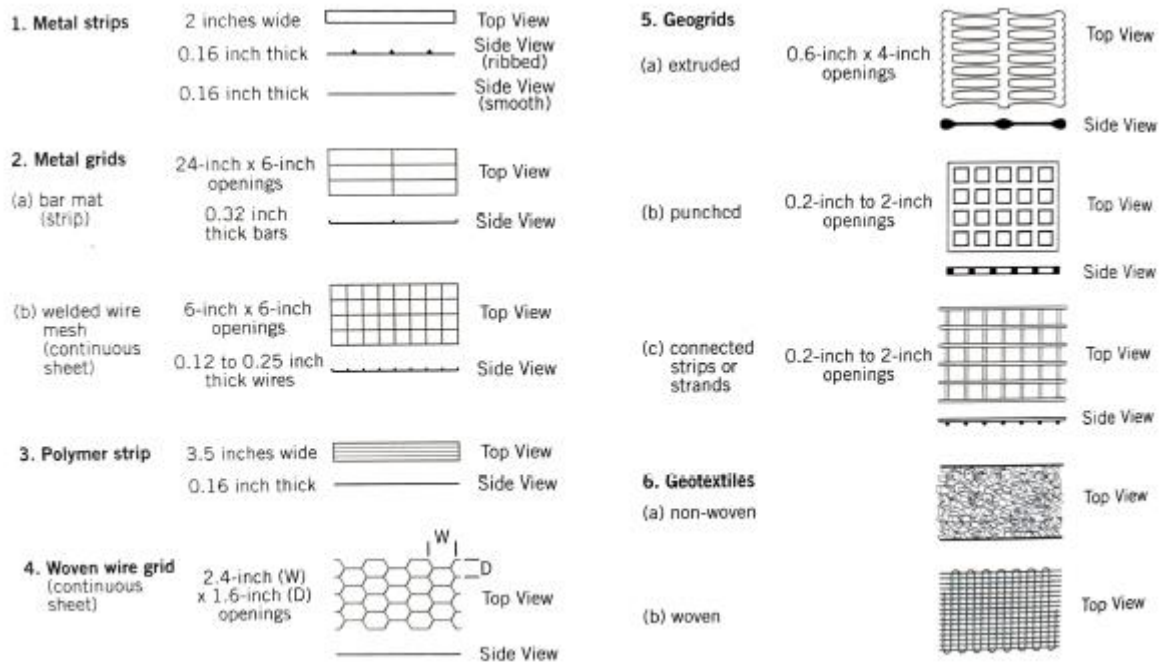

Figure 1.4 Types of soil reinforcement

There are various other techniques for the prevention of landslides such as Liquefaction mitigation techniques, slip surface strengthening by using isolated shear piles, earthworks, etc.

1.6 Prediction of landslides

Various warning systems are being developed and applied in field to minimize the damage inflicted by landslides by giving timely warning of slope failure. Early warning information of landslides and real time monitoring of dynamic deformation can significantly reduce the risk of possible casualties. From the viewpoint of prevention and mitigation of any catastrophe, this approach is very pivotal. A good warning system is one which is reliable and has a high level

of effectiveness. To make it more accessible, it should also be cost effective. Landslide prone areas can be monitored either remotely or by ground based sensor network. A combination of both will result in a system that can have a high degree of accuracy. Global Positioning System in combination with Remote Sensing Techniques such as laser scanning, imaging, etc. is frequently used for analyzing and monitoring purposes. But the ground based sensors have become the most important and most used technique for landslide monitoring and prediction as it is inexpensive compared to other methods. Certain parameters which are indicators of slope failure such as displacements, pore water pressures, tilt angles, saturation values of soil, etc. are monitored using special sensors or remote sensing techniques. A comprehensive warning system consists of:

1. Technology for monitoring and prediction
2. Communication of warnings to people
3. Human decision making

Also, the system should produce insubstantial false alarms so that the time and resources needed for intervention means can be avoided. When combined with successful measures to manage and mitigate landslides, a good prediction and forewarning system can dramatically decrease the harm caused by landslides. Unstable slopes necessitate remote monitoring systems that offer quick warning in the event of a failure. Advances in geotechnical/surveying instruments and data transmission methods now allow for simple and cost-effective monitoring of these slopes. For many unstable or potentially unstable slopes, remote, real-time monitoring of slope movement can be a useful strategy. Vibrating wire precipitations can be used to measure water levels. In-place inclinometers, tilt meters, extensometers, and autonomous survey systems can be used to measure lateral motions and deformation. All of these devices are linked to a data logger, which takes readings at certain intervals and delivers an alert or SMS if pre-determined values are exceeded. Depending on the circumstances, data can be transported utilizing cellular networks or radio frequency technology. An engineering geologist and consultant can use the data gathered to take remedial action and prevent landslip issues that are currently or will be in the future.

CHAPTER 2

LITERATURE REVIEW

2.1 GENERAL

This section presents an overview of research that has been done on testing of earth failure due to rainfall. The major part of it is focused on testing that is done in laboratory. Each paper has been discussed in concise manner, Images where required have also been given with proper references. The possible areas having potential for exploration are deduced from this survey and the objectives for this project are decided accordingly.

2.2 Literature Survey

Eckersley, 1990 [16] conducted a number of lab experiments on stockpiles of coking coal with a height of 1m. Water was made to infiltrate the coal slopes from top to toe to create instability as the level of water rose within the slope. These experiments were exercised in two series. The first series consisted of five experiments which were aimed to investigate the general character of instability, kinematics of failure and impact of inceptive density of coal on the failure process. The second series consisted of three experiments and the coal used was from other mines and not the mines that provided the coal for the first series. The second series of experiments were focused on examining the pore water and stress conditions exactly before and in the course of rapid flowslide failure.

Video cameras, piezometers, pore pressure transducers, temperature sensor probes, total stress cells and a data acquisition system were made use of for instrumentation.

Flowslides that occurred in the lab scale models were found to be very similar in nature to the ones that have taken place in stockpiles of coal in the mines. The saturation of the bottom of the slope and slow increment in the pore water pressure led to the instigation of flowslides. It was observed that mostly deep-rooted and usually retrogressive compounded failure governed the instability of the slope. Pore water pressures were generated swiftly after the initiation of sliding which resulted in the transformation of sliding mass to a stream of debris flowing abruptly. At last the stream of fast moving debris came to a halt and takes flat profile. These

experiments showed that the cause of failure initiation is not static liquefaction instead it is the outcome.

Tohari et al., 2007 [17] conducted a set of experiments on lab-scale models of slope soils. Rainfall induced slope failures were made by rainfall simulator. The intent of this study was to monitor thoroughly the slope failure initiation processes and the mode by which the slopes fail. Volumetric soil moisture content readings were also taken upon failure initiation. Special soil moisture sensor probes were installed at various locations to record the values. Residual granite soil and sandy soil were used in making the lab-scale models. They both fall into the category of sandy soils. Also the profile used for constructing a number of slopes, was straight and homogeneous in all experiments. Experimentation was focused to create instability in the slope models by raising the level of water, so that the process that initiates the slope failure can be explicated. It was observed that failure initiation was always marked by the formation of seepage area. This seepage area creates confined instability in the upper portion of the slope. This observation highlights the importance of tracking the emergence of seepage area. The volumetric moisture content of the portion of the slopes where the initiation of the confined failure occurred, was seen to almost reach the value of total saturation. But it was also observed that of all the portion of the slopes that led to comprehensive instability, most was unsaturated. This led to the conclusion that the change of moisture content levels in particular areas plays a vital role in predicting the instability.

Tu et al., 2009 [18] administered full scale field testing on a slope cut from instrumented loess by incorporating artificial precipitation. Loess is a kind of unsaturated soil. The site was on a cut slope of a highway loess on a plateau located in Northwest China. The yearly rainfall in that area is approximately 60 cm. The slope was made with six embankments from the surface of the plateau down to the road surface. The height of the embankments was not the same, but the angle of inclination of each rampart was 63°. The total height of the was 1855 cm and the overall angle was 42°. Soil moisture sensors, piezometers, tensiometers, water level sensors and rain gauge were equipped in the slope for instrumentation. These devices were installed in three separate capacities ST1, ST2 and ST3. Figure 2.1 shows the location of monitoring locations (Tu et al., fig.1a) [18]

Figure 2.1 Photograph of site showing monitoring locations

After approximately 2 years of monitoring under natural conditions, artificial precipitation was generated at the site using rainfall simulator in April 2007. Based on this study, it was found out that-

1. The active zone of absorption process was below the first 70 cm of the loess soil. The process of absorption and evaporation under low intensity rain (4cm/day), mainly occurred in this region. The depth of impact for this rainfall intensity was approximately 2m.

2. In case of heavy rainfall (12cm/day), the suction matrix decreased very quickly. The impact depth was 3m and the descent rate of matrix suction tended to slow down as depth increased.

3. As per the infiltration test, the matrix suction within a depth of 3 meters from the ground, after 9 days of infiltration was nearly zero. Therefore, the amount of precipitation accumulated during the previous 9 days was important for the stability of the slope. So, soil permeability should be considered to analyze and predict the slope failures caused due to rainfall.

Huang et al., 2009 [19] performed three extensive flume tests by failing the soil slopes through simulated rainfall. Their motive was to study the response of water on piezometer and to gain greater understanding about internal soil moisture. Local soil was used to make soil slopes. The soil was categorized as Silty Sand in UCS system. The initial moisture content for the experiments was kept in the range of 5% to 10%. To measure the volumetric moisture content, twelve moisture sensors were installed. The moisture data was accessed using a data logger. Six piezometers were also installed to measure the pore water pressures. The location of these instruments is shown in figure 2.2 (Huang et al., fig. 4b) [19].

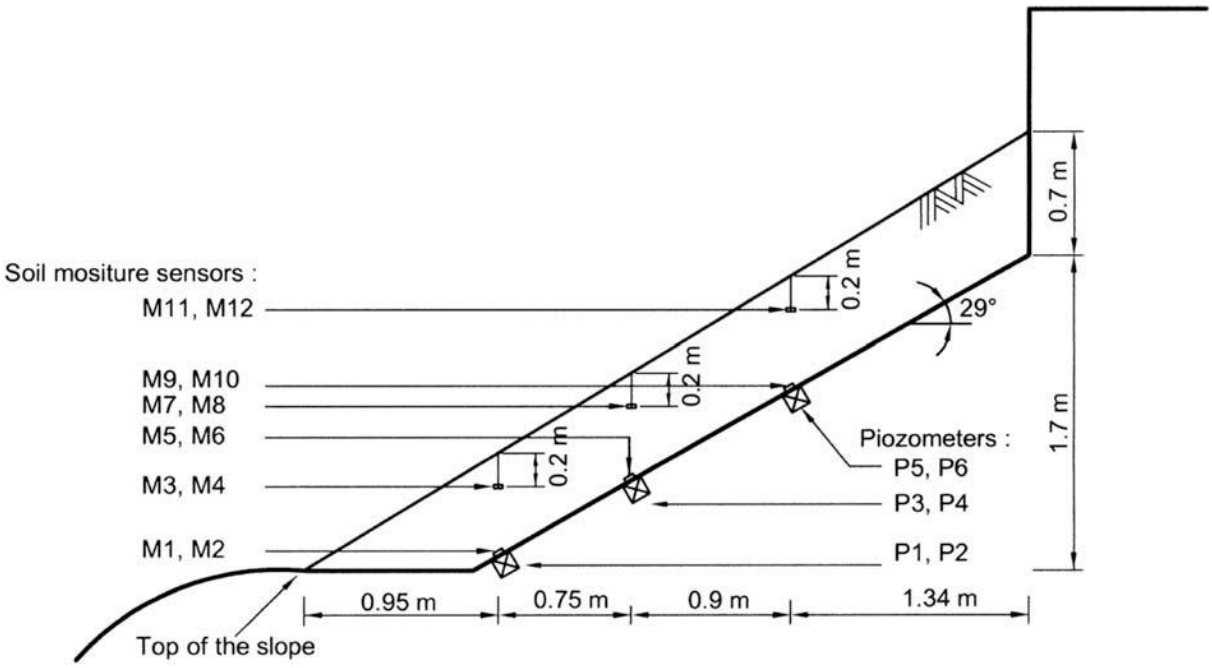

Figure 2.2 Side view of locations of soil moisture sensors and piezometers

The outcome of these experiments brings out the fact that response time on the basis of both pore water pressures and moisture content readings, at the juncture between soil and bedrock can be a constructive sign of shallow earth slope failures. This paper suggests that criteria based on internal response time rather than the traditional approach of using rainfall thresholds can manifest better accuracy in forecasting shallow slope failures.

Catane et al., 2011 [20] examined the physical changes that occurred in the lab based soil slope models, when they were exposed to instability through simulated infiltration of

groundwater. An upslope tank was used to make water penetrate to the slope's toe laterally. Homogeneous sample of porac sand consisting of ferromagnesian minerals, plagioclase and quartz was used to make slopes. Tilt sensors were installed at upper portion and toe portion of slope models. For additional visual monitoring, two video cameras were also set up. In this study it was observed that when water infiltrated slowly into soil mass, the area of toe displayed the most notable sensor reading changes and also visual changes. The foremost visual change was the bulging of toe area causing seepage there. This seepage led to localized failure of soil. After that piping was observed which led to retrogressive failure. Finally, before the major portion of soil mass failed, tension cracks were also observed. Also it was noteworthy that the instrumental changes in the upper portion of the models were not as significant as that of toe area. However, the features of deformation did appear but only after the start of the failure.

Wicaksana et al., 2014 [21] carried through a laboratory based experiment to explore the mechanisms and consequences of slope failure using a centrifuge. The basis of modelling in a centrifuge is that the stresses in the model and the prototype are same at the same points in the geometry of the both. Bucky (1991) [22] proposed an approach to carry out physical modelling in centrifuge: "To generate the same unit stress at corresponding location of the small scale model that are present in the prototype, the weight of the model material should be increased in the same ratio as the model scale is decreased corresponding to the prototype. The effect of weight gain can be achieved by placing the model in a suitable rotating device and applying centrifuge force".

The slope model was prepared with clayey-silt of height 15cm and slope angle of 35°. The base layer was 10 cm in depth. The failure mechanism of collapsed slope, was explored by spinning the centrifuge at various degrees of acceleration and water content. The maximum value of centrifuge acceleration was 3.8g to which slope model was subjected and the water content variations were 0, 5, 10 and 15%.

The mode of failure for every case found to be circular. With an increase in water content, the value of exerted centrifugal acceleration to kick-start the slope collapse also increased. According to the findings of this study, centrifugal acceleration, cohesiveness and failure time

were all linearly proportional with the moisture content lower than OMC. In contrast, the angle of internal friction and the quantity of crumbled material were non-linear with moisture content.

Wu et al., 2015 [23] carried out a series of lab tests on loose soil slopes to observe soil deformities and failures. On the basis of the test results, potential processes leading to these deformations were expounded. Model flume was used to prepare test slopes. Rainfall simulation system was used to simulate rainfall, which could spray rainwater with varying intensities. Small sized sensors were used for the determination of pore water pressure and soil moisture content. Landslide earth of Wenchuan Earthquake region was the source of soil for the tests. This soil falls into the category of sand. Model slope angles of 30° and 37° were used for these tests.

In these experiments, the deformation of slope was triggered due to permeation of water leading to formation of cracks in the slope at its trailing edge. The pore water pressure and moisture content increased promptly at the trailing edge after the water permeated into these cracks. The failures were closely linked with the gradient of the slope and the intensity rainfall. With decreasing slope angles, the wetting front developed more quickly and the sliding plane became deeper. This was due to the reason that on moderate slopes it was easier for water to permeate to a deeper area. Also, long rainfall periods with lesser intensity gave rise to larger depths of sliding plane which generates a larger landslide.

Chueasamat et al., 2018 [24] did a course of investigational experiments by utilizing 1g physical models of slopes. Their main motive was to experimentally study the effects of density of surface sand layer and intensities of rainfall on slope failures because of rainfall. The 1g physical models were made of Kasumigaura lake in Japan and a type of silty sand termed as DL clay. Every single model of slope composed of a permeable surface sand layer of little depth on a comparatively firm base with an angle of 45°. This orientation is similar to standard natural slopes that are failure prone. Nine scenarios with distinct combinations of surface sand layer densities and intensities of rainfall were tested in totality. These different cases are summarized in the table 2.1 (Chueasamat et al., table 3) [24].

Table 2.1 Initial conditions of slope model tests

Case	Rainfall intensity, I (mm/h)	Relative density, D_r (%)	Water content, w (%)	Dry density, ρ_d (g/cm^3)	Degree of saturation, S_r (%)	Initial void ratio, e_0
1	25	0	10.6	1.350	28.7	0.994
2	25	25	10.0	1.423	30.2	0.892
3	25	50	9.8	1.498	33.1	0.797
4	50	0	11.0	1.345	29.6	1.001
5	50	25	10.0	1.423	30.2	0.892
6	50	50	10.0	1.495	33.6	0.801
7	100	0	12.9	1.322	33.5	1.036
8	100	25	10.0	1.423	30.2	0.892
9	100	50	9.8	1.498	33.1	0.797

There were two types of rupture observed – surface slip faults and retrograde rupture. The failure of slope was clearly influenced by precipitation intensity and the density of sand layer. When the Relative density was less and intensity of rainfall was high, surface slip occurred and when the case was opposite, retrograde failure occurred. For the surface slip rupture, the occurrence of first rupture was followed by a large shallow rupture. This may be primarily caused by a decrease in the shear strength due to saturation of entire sand layers. For retrograde failures, a small series of failures occurred after the first failure. This type of failure could be primarily caused by a reduction in effective stress, as the areas where failure occurred were fairly consistent with those monitoring excessive pore water pressure.

Some similar features were also observed in the course of failure process. The time at which the maiden failure occurred, decreased when both sand layer density and intensity of rainfall increased.

Zhang et al., 2109 [25] performed a series of flume tests on loess soil with vertical and terraced slope types. They monitored various parameters such as water content, pore pressure, matric suction, etc. as the artificial precipitation was made to fall on the slope models at a steady intensity of 12mm/h. Rainfall infiltration led to an increase in level of volumetric moisture content and a decrease in matric suction. The pore water pressure responded later than the water content and matric suction. The failure of slope occurred when the VMC was at its highest level and matric suction was at its lowest level. In vertical slope, consistent rainfall for short period led to sudden shallow failure, whereas in terraced slope, consistent rainfall for long period led to slowly progressing failure. Also, for short period rainfall, failure pattern was of sliding of

blocks in different stages and for long period rainfall, failure pattern was observed to be of flow slide.

Paswan & Shrivastava, 2022 [26] did laboratory based physical modelling to investigate the process of failure of slope in the study region by simulating the environment present in that area. They also performed numerical modelling with the help of GeoStudio software for evaluating the parameters of seepage and stability of slope. The study area was located along NH-5, in the vicinity of Sutlej river, in Jhakri village of district Shimla in Himachal Pradesh, India. The slope that was investigated had an elevation of 55 meters above the ground and had an angle of 35°. The slope material was graded as silty-sand. The actual slope was scaled down for flume testing in laboratory and the lab model was similar in nature with that of actual slope as per the similar theory. Precipitation was simulated on the model slope in accordance with actual rainfall that occurred in the study area.

The FOS was determined to be 1.23 on GeoStudio. This implied that the slope was stable before the rainfall was applied on it. After that rainfall was simulated on the slope with an intensity of 30mm/h. Percolation of water took place after rainfall depth of 30mm was achieved. Also, on the face of slope, erosion and weathering could be seen. With the continuation of rainfall, as the rainfall depth reached 50mm, drainage gullies started to form. The soil slope failed at rainfall depth of 80mm. After the rainfall, the FOS was determined to be 0.626 on GeoStudio. This study concluded with the finding, that rainfall depth of 80mm can be used as a threshold for predicting landslide in that particular slope.

2.3 Research Gaps

- The physical and instrumental behaviour of different soils vary when subjected to water infiltration.
- There is a lack of literature that specifically focuses on response of soil on steep slopes.
- Very few researches tell about the degree of soil saturation at the time of slope failure.
- The quantitative effect of retaining wall on FOS of the slope may be studied.

2.4 Research Objectives

- Prepare lab scale models of slopes from locally available soil and carry out slope stability analysis of these slopes on GEO5 software.
- To investigate the failure pattern of soil slopes under artificial rainfall.
- To determine the saturation values at which the slopes fail.
- Design a retaining wall for an in situ slope and to compare the values of FOS for slope stability before and after the construction of retaining wall.

CHAPTER 3

DESIGN & METHODOLOGY

3.1 Methodology

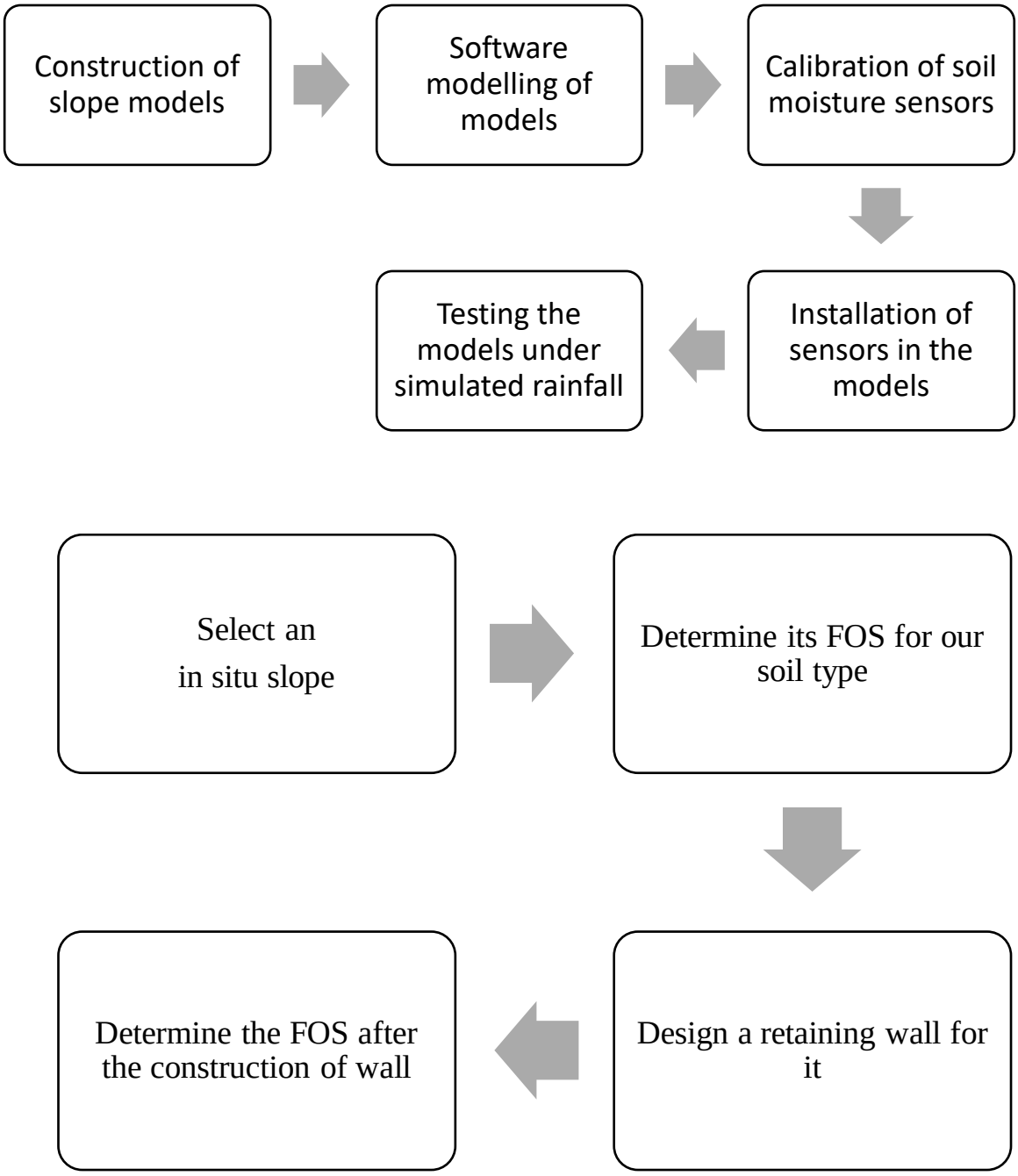

3.2 Material used

- Soil

The soil that was used to make slope models was procured from the banks of a stream that flows in village Domehar near university campus.

Figure 3.1 Soil used for experimentation

The properties of the soil sample for preparing model slopes are given in the table below.

Table 3.1 Properties of soil sample

Specific gravity	2.72
D10	0.15 mm
D30	0.20 mm
D50	0.24 mm
D60	0.30 mm
Coefficient of uniformity, Cu	2
Coefficient of curvature, Cc	0.9

Friction angle, φ	38°
Cohesion value	0
Bulk mass density	1.4 (g/cm³)
Dry mass density	1.386 (g/cm³)
SBC	150 (KN/m²)
Angle of repose	35°

- Water spray gun

An adjustable water spray gun was used to simulate rainfall over the models. The amount of water coming out of it was first adjusted by using a rain gauge.

Figure 3.2 Adjustable spray gun

- Flume boxes

Flume boxes open from front side were used to makes slopes inside them. They had metal sheet on base and plexiglass on three sides so that failure process can be observed easily.

Figure 3.3 Flume box

- Soil moisture sensors

Capacitive sensing is used to assess soil moisture levels in these Capacitive soil moisture sensors. They provide instantaneous soil moisture data by embedding them into the soil. Sensor module has an integrated voltage regulator and an operational voltage range of 3.3-5.5V. Sensor low-voltage MCUs. [27]

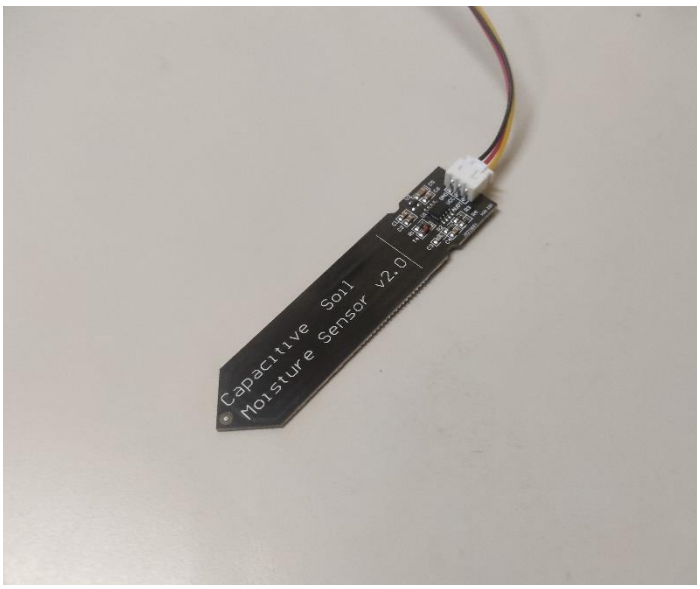

Figure 3.4 Capacitive soil moisture sensor

- Micro Controller Unit

The ESP32 is used as a MCU for signal reception from soil moisture sensors and signal transmission to IoT platform. It is an affordable, low-energy microcontroller which has Wi-Fi and bluetooth inbuilt. It comprises of an integrated antenna and RF balun, plus a power amplifier, low-noise amplifier, filter, and a power management module. The complete design occupies the minimal printed space on circuit board. This board is equipped with 2400 MHz dual-mode Wi-Fi and bluetooth chips from TSMC 40nm with low power technology, having the best power and RF attributes. It can be used for a wide range of functions. [28]

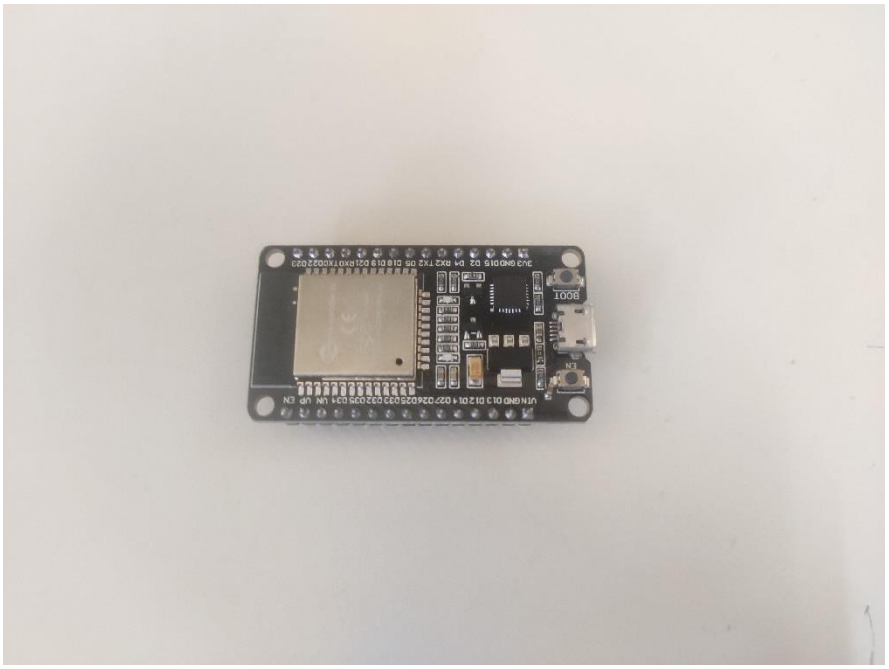

Figure 3.5 ESP 32

3.3 Software used

- ThingSpeak

ThingSpeak is an IoT Cloud platform that allows users to communicate sensor data to the cloud. MATLAB or other tools can also be used to interpret and visualize data [29]. Readings of soil moisture sensors were accessed using this service.

- Geo5 software

The slope stability analysis of model slopes was done in this software. The verification of retaining wall design and calculation of FOS for it was also done on this software.

3.4 Description of model slopes

Two slopes were prepared for lab testing, with slope angles of 60° and 70°. The maximum dimensions of 60° slope tank were 0.85 x 0.75 x 0.9 m and for 70° slope tank they were 0.7 x 0.4 x 0.7 m. The tanks had a metal sheet at base and plexiglass sheet on three sides. They were open from the front and top side so that the slopes can be prepared with ease inside of them and also installation of sensors can be effortless. The soil in the slopes was targeted to achieve a bulk mass density of 1.4 g/cm³. The soil was placed inside the boxes in layers to maintain homogeneity of the slopes and the slopes were uniform throughout. The effect of vegetation was not considered. Three soil moisture sensors were installed in the slopes to record moisture content. Sensor number 1 was placed at a depth of 20 cm from top. Sensor number 2 and 3 were installed near the toe and top end of slope respectively. The figure below shows the dimensions of soil slopes with the location of soil moisture sensors.

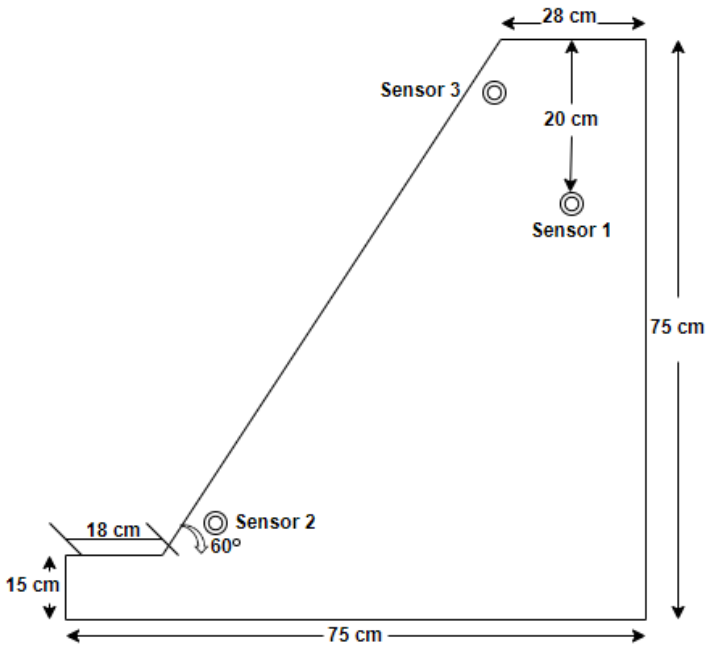

Figure 3.6 (a) Location of soil moisture sensors in 60° slope model

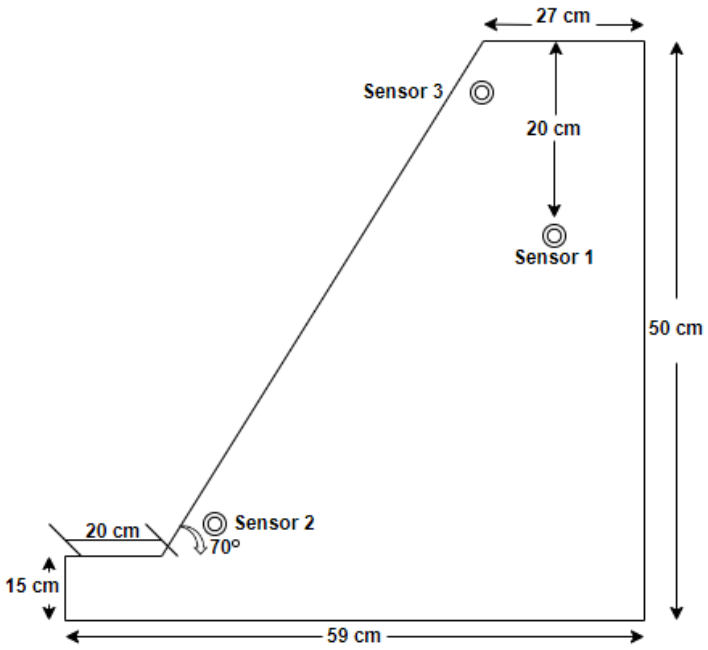

Figure 3.6 (b) Location of soil moisture sensors in 70° slope model

The figure below shows the sensor network.

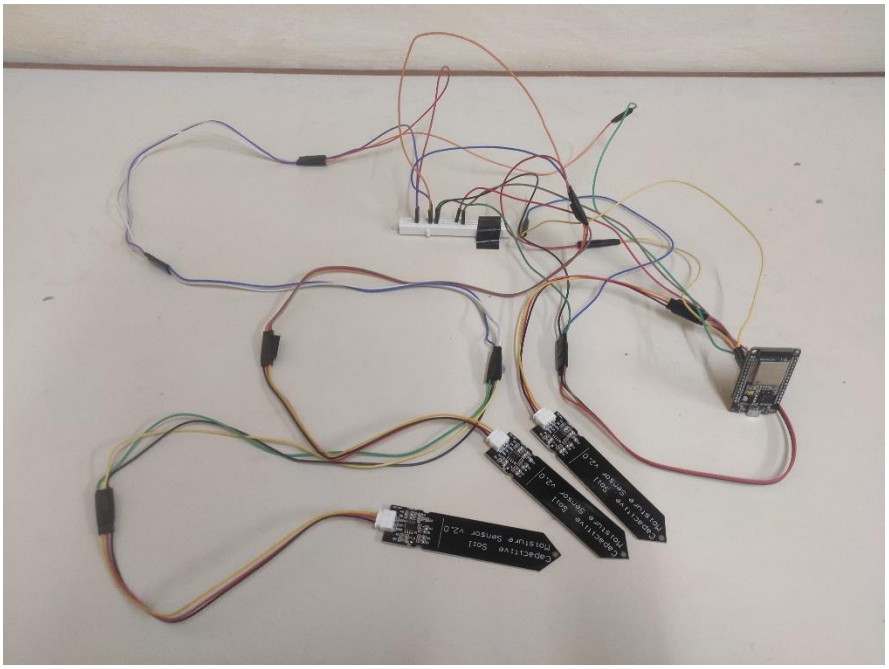

Figure 3.7 Sensor network

3.5 Description of in situ slope

The slope for which the retaining wall is to be designed is located on NH-5 in village Jhakri of district Shimla. The slope is situated close by river Sutlej which is also the watershed area of slope. The slope is 55 meters in height with 30° angle of slope [26]. The material of this slope is considered to be our investigational soil and the retaining wall is designed accordingly.

3.6 Design of cantilever retaining wall

4 m height is to be retained above GL, backfill inclination (δ) is 30°

Unit weight of the soil (γs) is taken as17 KN/m³, Internal friction angle is (φ) is 38°

Friction coefficient between soil and concrete (μ) is 0.5, SBC is 150 KN/m²

Using M20 & Fe 415

Step 1- Determine the depth of foundation

$$\text{Depth} = \frac{qa \times [1-\sin\varphi]^2}{\gamma s \times [1+\sin\varphi]^2} = 0.605 \text{ m}$$

Assume depth (H) of 1 m

Overall depth = 4+1 = 5 m

Step 2- Selection of initial sizes

Width of footing (B) should be 0.5H to 0.7H

Taking B = 3 m

Width of Heel should be 0.5B

= 1.5 m

Base Slab thickness = H/12 = 420 mm

Thickness of stem at top ≈ thickness of stem at base/2 = 210 mm

Height of Stem = H-thickness of base slab

Adopt = 4580 mm

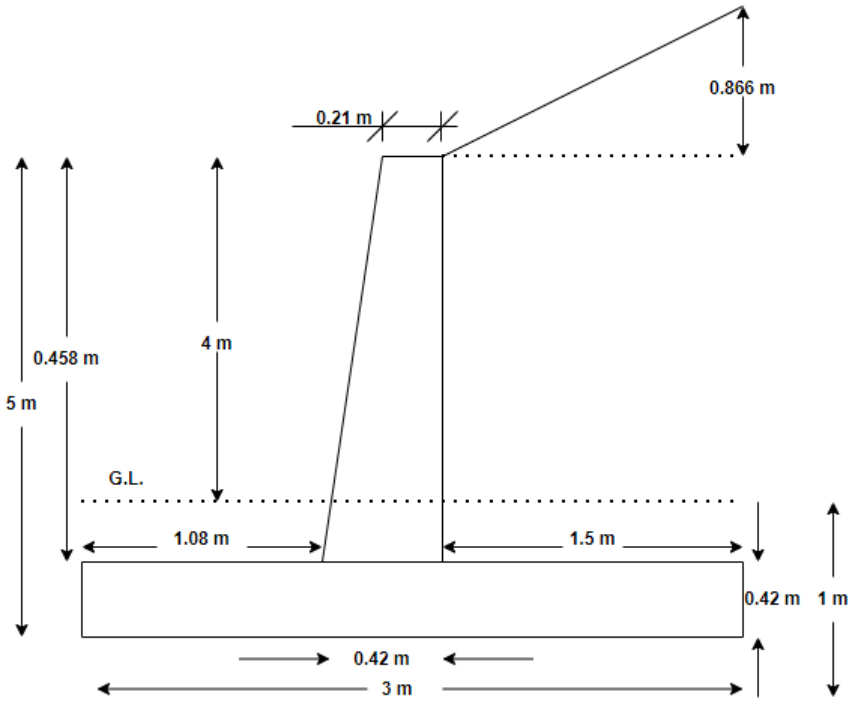

Figure 3.8 Dimensions of retaining wall

Step 3- Computation of forces and moments acting on the wall

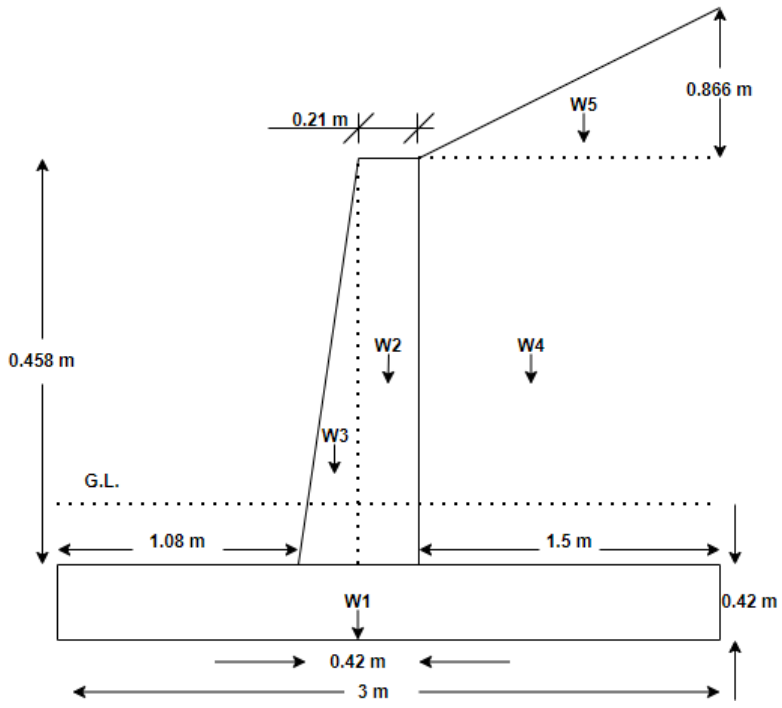

Figure 3.9 Various forces on retaining wall

Table 3.2 Forces & Moments acting on the wall

No.	Annotation	Entity	Force (KN)	Distance of C.G. from heel (m)	Moment (KNm)
1	W1	Base Slab	31.5	1.5	47.25
2	W2	Rectangular portion of stem	24.045	1.605	38.56
3	W3	Triangular portion of stem	12.0225	1.815	21.82
4	W4	Rectangular portion of backfill	116.79	0.75	87.6
5	W5	Inclined portion of backfill	11.04	0.5	5.52
			ΣF = 195.39		ΣM = 200.75

Step 4- Calculate the earth pressure

Coefficient of active earth pressure (ka) = $\frac{\cos\delta - \sqrt{\cos^2\delta - \cos^2\varphi}}{\cos\delta + \sqrt{\cos^2\delta - \cos^2\varphi}} \times \cos\delta$

ka = 0.358

Coefficient of passive earth pressure (kp) = $\frac{1+\sin\varphi}{1-\sin\varphi}$

Kp = 4.2

Force because of active earth pressure (Pa) = ka $\boldsymbol{\gamma s}$ (H′)/2

where, H′ = 5+0.866 = 5.866 m

Pa = 1.4.7 KN

Horizontal component of Pa = Pa cos δ = 90.67 KN

Vertical component of Pa = Pa sin δ = 52.35 KN

Step 5- Check for stability

Factor of safety against overturning

$$\frac{0.9 \times \text{Stabilizing moment (Mr)}}{\text{Overturning moment (Mo)}} > 1.4$$

Mo = 90.67 x H′/3 = 177.29 KNm

Resultant vertical force distance from heel (x)

x = ΣM/ ΣF = 1.027 m

Stabilizing moment about toe (Mr) = ΣF (B-x)

Mr = 385.5 KNm

Therefore, FOS against overturning 0.9 x 385.5/177.29

1.9 >1.4

Hence the wall is safe against overturning

Step 5- Calculation of soil pressure below the base slab

$$\text{Eccentricity (e)} = \frac{\Sigma M + \Sigma Mo}{\Sigma F} - \frac{B}{2} < B/6$$

e = 0.43 < 0.5 m

$$\text{Maximum pressure (P1)} = \frac{\Sigma F}{B}\left(1 + \frac{6e}{B}\right)$$

P1 = 121.1418 KN/m² < SBC of soil (150 KN/m²)

Hence Satisfactory

$$\text{Minimum pressure (P2)} = = \frac{\Sigma F}{B}\left(1 - \frac{6e}{B}\right)$$

P2 = 9.1182 KN/m²

Step 6- Check for stability against sliding

$$\text{Factor of safety against sliding} = \frac{0.9 \times \text{Resisting force (F)}}{\text{Sliding force (Pa cos } \delta)} > 1.4$$

Resisting force (F) = μ ΣF

F = 97.695 KN

Therefore, FOS = 0.9 x 97.695/90.67 = 0.96

0.96 ≯ 1.4

Hence shear key need to be provided.

Step 6- Design of shear key

Considering a shear key of 300 mm x 400 mm at a stretch of 1100 cm from toe

The effect of shear key is to develop passive resistance over a depth of h2

For calculating the passive pressure under the toe, top overburden of 300 mm is normally neglected

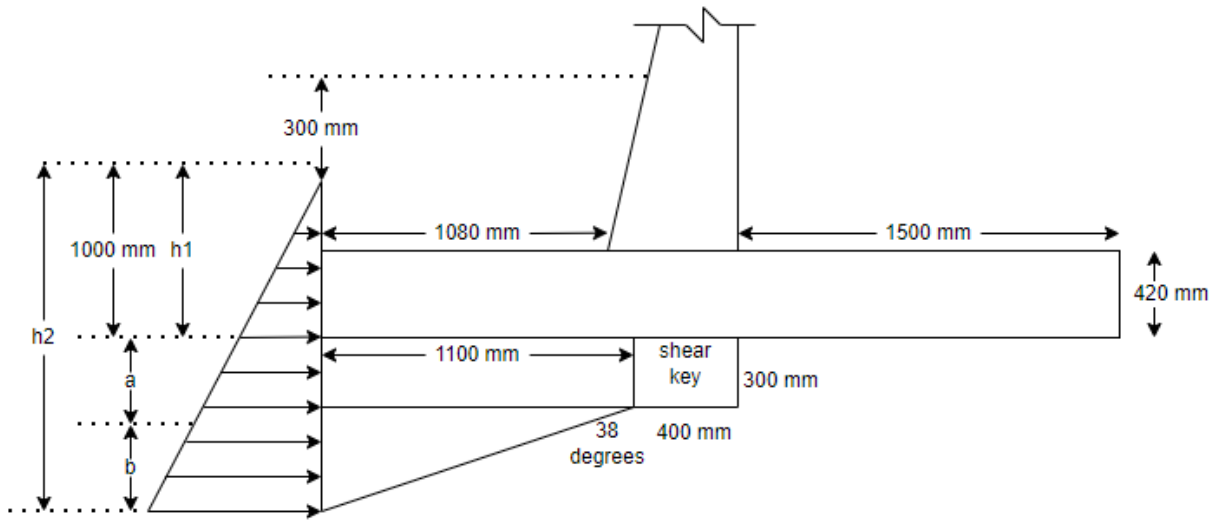

Figure 3.10 Pressure diagram for shear key

Hence, h1 = 1-0.3 = 0.7 m

a = 300 mm

Also b = 1.1 x tan 38° = 0.859 m

Passive earth pressure (Pp) = $kp\ \gamma s\ \frac{(h1+a+b)^2}{2} - kp\ \gamma s\ \frac{h1^2}{2}$

Pp = 105.877

FOS against sliding

$$\frac{0.9\ (F+Pp)}{Pa\cos\delta} > 1.4$$

2.02 > 1.4

Now it is safe against sliding

Step 7- Design of toe slab

Pressure due to dead-weight of toe slab per m^2 = 2.5 x 0.42 = 10.5 KN/m^2

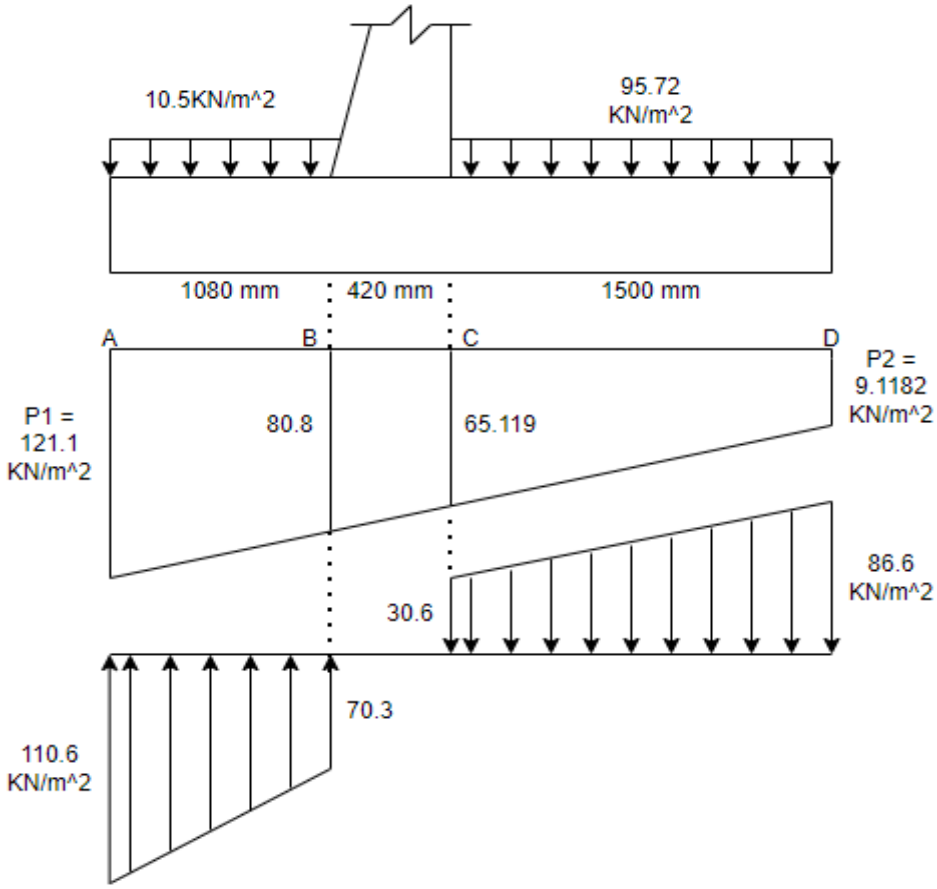

Figure 3.11 Pressure diagram for Toe and Heel

Final upward pressure varies from 110.6 KN/m^2 to 70.3 KN/m^2

Now, assuming 16 mm bars and clear cover of 7.5 cm

Design BM at the face of stem (Mu)

$$1.5\ \{[70.3 \times \frac{(1.08)^2}{2}] + 0.5[(110.6-70.3) \times (1.08)^2 \times 2/3]\} = 98.5\ KNm$$

Now $Mu = 0.85\ fy\ Ast\ d\ eff\ (1 - \frac{Ast\ fy}{bd\ fck})$

Substituting the values, we get $Ast = 860\ mm^2$

Spacing $= \frac{\pi/4 \times 16^2 \times b}{Ast} \approx 240$ mm

Therefore, provide 16 mm bars @ 240 mm c/c

Distribution steel = 0.0012 x 1000 x 420 = 504 mm^2/m

Taking 10 mm bars, Spacing = 785000/504 ≈ 150 mm

Providing 10 mm bars @ 150 mm c/c

Developmental length (Ld) = 47 x 16 = 752 mm beyond the face of stem

Step 8- Design of Heel

Pressure due to-

1. Soil = 17 x (4.58+0.866/2) = 85.221 KN/m^2

2. Self-Weight = 25 x 0.42 = 10.5 KN/m^2

Total = 95.721 KN/m^2

Net downward pressure varies from 30.6 KN/m^2 to 86.6 KN/m^2 (see fig. 3.10)

Design BM at the rear face of stem (Mu)

$1.5\ \{[30.6 \times (1.5)^2] + [0.5(86.6-30.6) \times 1.5^2 \times 2/3]\} = 114$ KNm

Now $Mu = 0.85\ fy\ Ast\ d\ eff\ (1 - \frac{Ast\ fy}{bd\ fck})$

Substituting the values, we get $Ast = 998\ mm^2$

Adopt $Ast = 1000\ mm^2$

Taking 16 mm bars, Spacing = 201000/1000 ≈ 200 mm

Provide 16 mm bars @ 200 mm c/c

Distribution steel

Provide 10 mm bars @ 150 mm c/c

Also, the bars should extend at least by distance 1.3 x Ld = 1.3 x 47φ = 978 mm beyond the rear face of stem

Step 9- Design of Stem

Assuming 20 mm bars and clear cover of 5 cm

d eff = 420-50-20/2 = 360 mm

Force due to active earth pressure (Pa)

Pa = ka γs (H′)/2

where H′′ = 4.58+0.866 = 5.446

Pa = 90.25 KN/m

Horizontal component = Pa cos δ = 78.16 KN/m

Design BM

Mu = 1.5 x 78.16 x H′′/3 = 212.8 KN/m

Now $Mu = 0.85 fy Ast d eff \left(1 - \frac{Ast\ fy}{bd\ fck}\right)$

Substituting the values, we get Ast = 1830 mm²

Provide 20 mm bars, spacing = 314000/1830 ≈ 170 mm

Provide 20 mm bars @ 170 mm c/c

Curtailment of Reinforcement

Curtail 50% steel from top

$\frac{x}{4580} = \frac{1}{2}$

x = 3.28 m

Actual point of cut-off = 3.28-Ld (47x20) = 2.3 m from top

Hence, double the spacing for 2.3 m length from top

Distribution steel = 0.0012 x 1000 x 315

where, $315 = \frac{420+210}{2}$

≈ 380 mm²/m

Providing 190 mm² on each face and using 8 mm bars,

Spacing = 260 mm

Provide 8 mm bars @ 260 mm c/c on tension face of stem wall

A mesh of 8 mm bars @ 260 mm c/c is given on compression face of stem wall

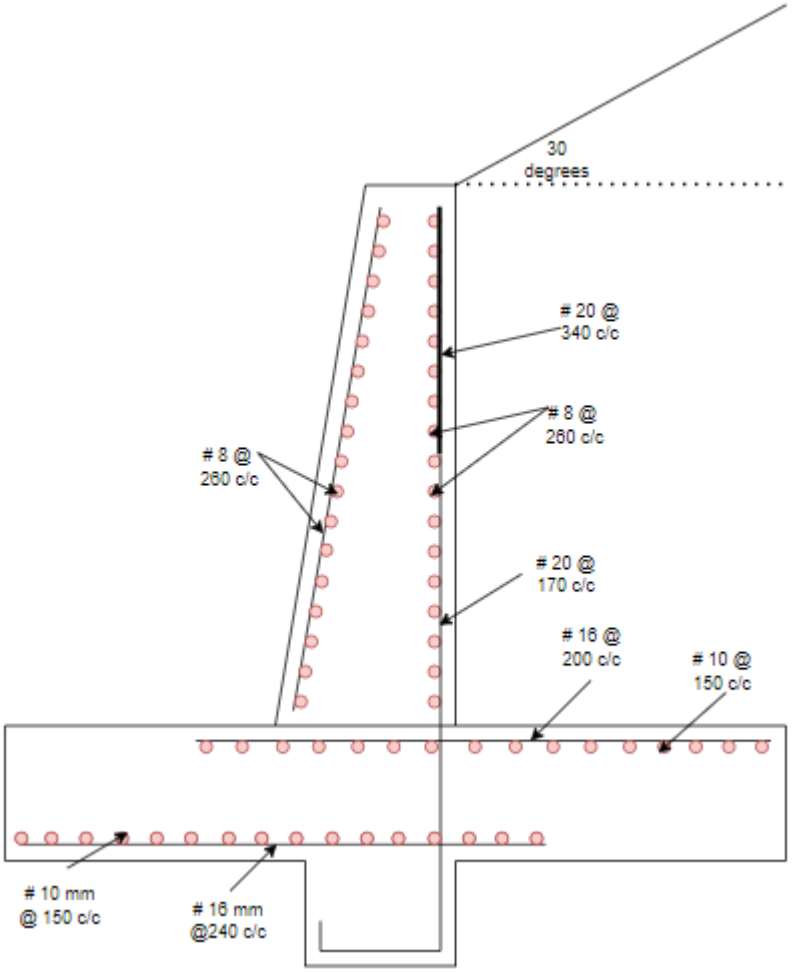

Figure 3.12 Reinforcement details

CHAPTER 4

RESULTS

4.1 Stability Analysis of model slopes

The stability analysis of model slopes was carried out on Geo5 software to determine the FOS and the location of most critical slip surface. The Bishop method which takes into account the forces on the edges of each slice, was used to calculate the FOS. The FOS is the ratio of maximum shear strength of the soil on the considered surface to the shearing resistance mobilized on that surface [30]. After the analysis FOS for 60° slope model came out to be 0.75 and the FOS for 70° slope model came out to be 0.71. It shows that the both the slopes are highly unstable as the FOS < 1. The most critical slip surface is shown in figure below.

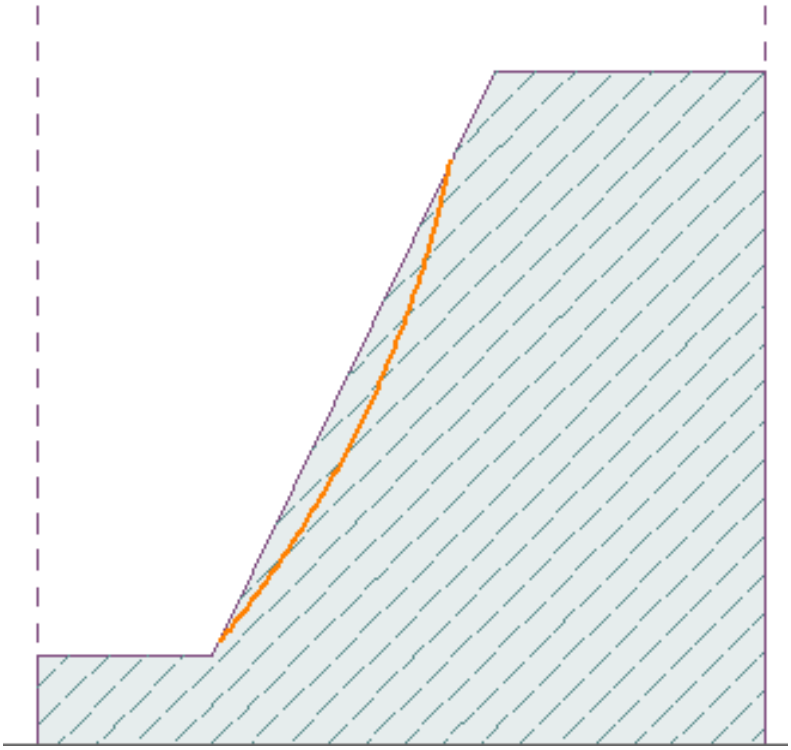

Figure 4.1 (a) Most critical slip surface for 60° slope model

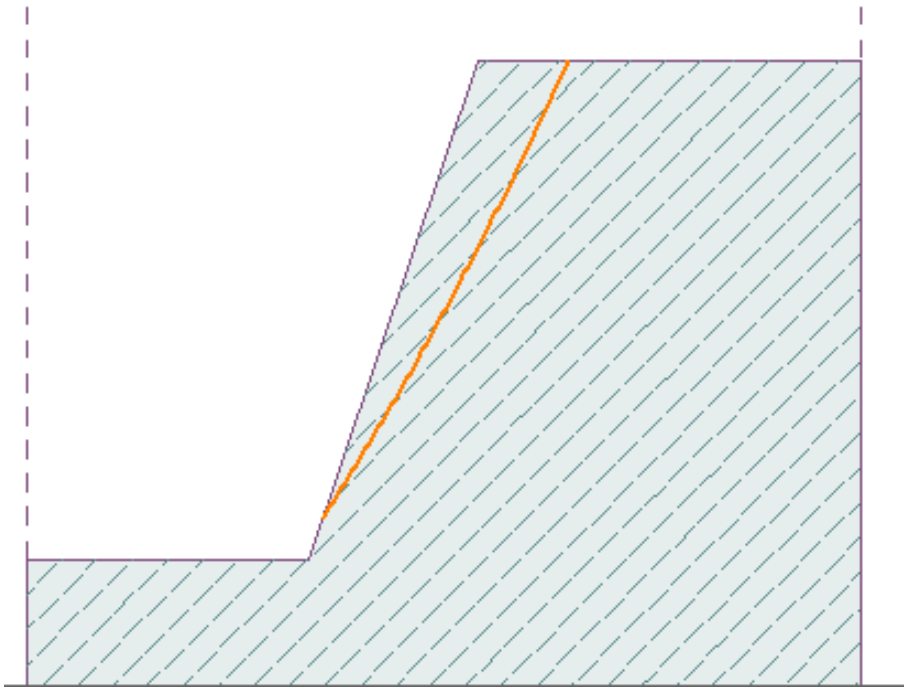

Figure 4.1 (b) Most critical slip surface for 70° slope model

4.2 Observations made from rainfall testing

The rainfall was simulated over the slope models at an intensity of 4mm/min and it is categorized under high intensity rainfall. Every effort was made to take use of every resource and simulate proper rainfall but it was not possible to bring the value of rainfall intensity further down due to lack of proper rainfall simulator. Nevertheless, it was made sure that falling rain droplets covers as much area as possible and fall evenly on the slope models.

4.2.1 60° slope model

- Before the start of artificial precipitation, the value of moisture content was determined with the help of moisture sensors and it was approximately 1% for the whole of soil slope model. Figure 4.2 shows the picture of slope model just when the precipitation was started.

Figure 4.2 Soil profile at the beginning of rainfall

- After continuous rainfall for about 4.5 minutes a big tension crack formed at the top edge of the slope. The figure below shows the tension crack developed in the slope.

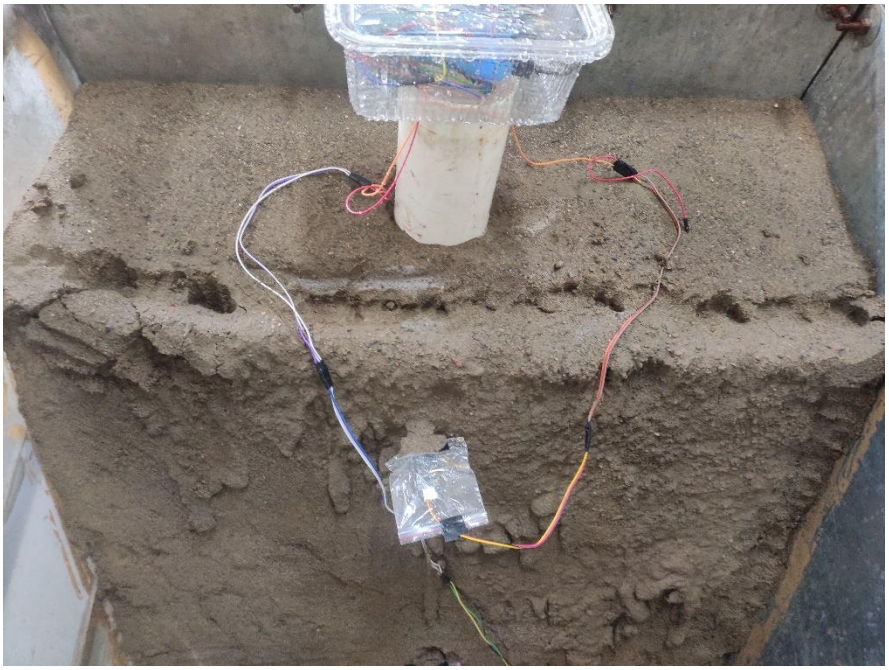

Figure 4.3 Tension Crack

- After approximately t = 7 minutes the slope failed and the mode of failure was observed to be sliding failure. Figure 4.4 shows the failed slope. The maximum slide depth was found out to be 8 cm. Figure 4.5 a & b shows the side profile of slope before and after failure.

Figure 4.4 Failed slope

Figure 4.5 (a) Side view of model before failure

Figure 4.5 (b) Side view of model after failure

- The recorded values of moisture content in various moisture sensors at the time of failure are present in figure no. 4.6.

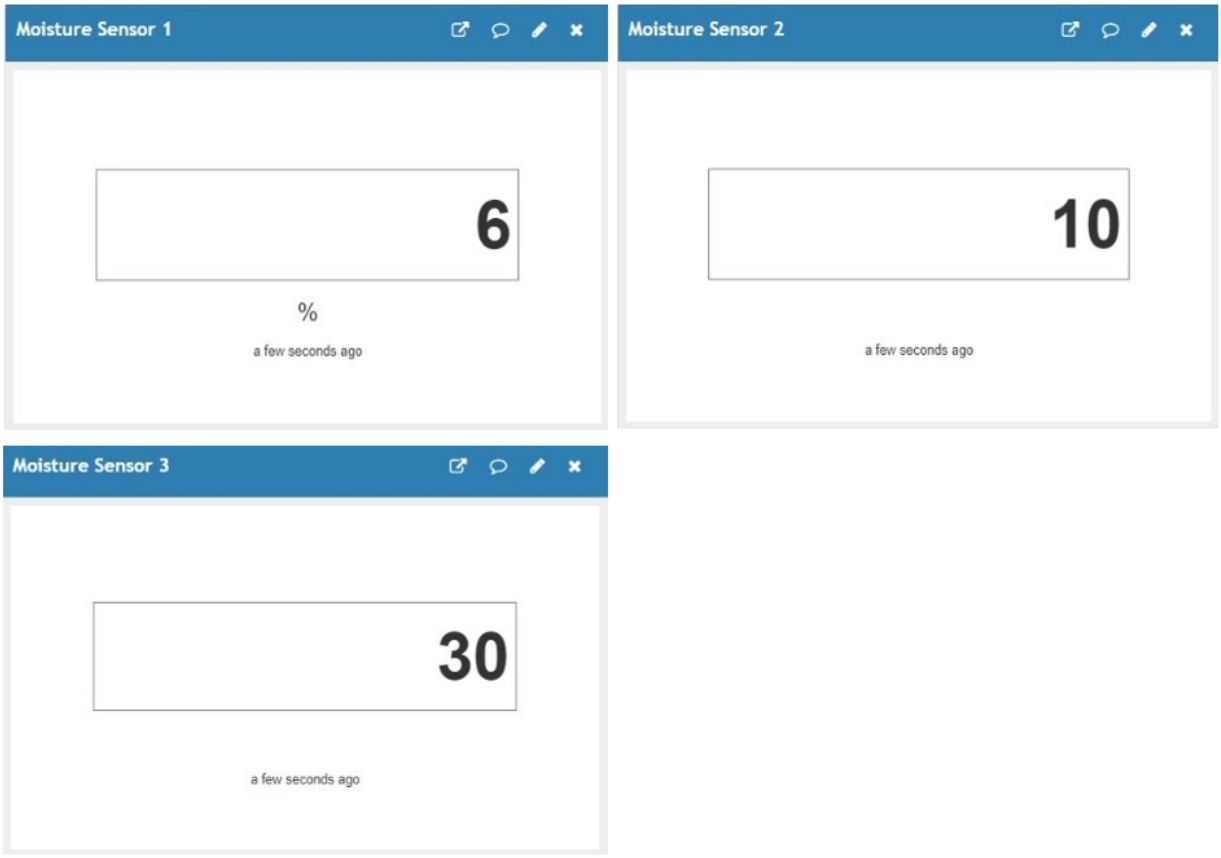

Figure 4.6 Moisture content values at the time of failure

- Using relations these values are converted into corresponding values of degee of saturation and are given in the table below.

Table 4.1 Values of degree of saturation

Location	Value of degree of saturation
Moisture Sensor No. 1	16%
Moisture Sensor No. 2	27%
Moisture Sensor No. 3	84%

4.2.2 70° slope model

- Initially, moisture content was at 1% for this model as well. Figure 4.7 shows the view of the model.

Figure 4.7 Soil profile before rainfall

- After 6 minutes of uninterrupted rainfall the slope collapsed by sliding. The figure below shows the collapsed slope.

Figure 4.8 Collapsed slope

- Figure 4.9 a & b shows the side view of slope before and after failure. The sliding depth was observed to be at a peak value of 6 cm.

Figure 4.9 (a) Side view of slope before failure

Figure 4.9 (b) Side view of slope after failure

- The values of degree of saturation of soil at sensor locations, converted from moisture content levels are shown in table below.

Table 4.2 Degree of saturation at different locations

Location	Value of degree of saturation
Moisture Sensor No. 1	15%
Moisture Sensor No. 2	24%
Moisture Sensor No. 3	79%

4.3 FOS comparison for in situ slope

The FOS of the in situ slope with soil properties as given in section 3.5, came out to be 1.36 using Bishop method on Geo5. This suggests that the particular slope is stable on its own as the FOS is greater than 1. This is also clear from the fact that the angle of repose of the used soil is 35° and the inclination of this slope is at an angle of 30°. The FOS was again calculated on software using the same method after the slope was reinforced with cantilever retaining wall. It was deduced to be 1.53. This shows that the stability of the slope has improved for sure, as there is a notable increase in the factor of safety for soil stability.

CHAPTER 5

CONCLUSIONS AND FUTURE SCOPE

5.1 RESEARCH OUTCOMES

- In both the test slopes, the soil mass failed by sliding. It was noticed that whole of the slopes failed and the slopes did not fail in parts. The mechanism of failure was almost similar in both slopes and can be explained as follows: As the rainwater falls on the surface of slopes the soil becomes saturated and its weight starts to increase. Increase in weight of the soil causes the soil to start sliding as it is steep and this decreases the stability of the slope. This leads to the formation of tensile stresses as the soil separates from surrounding soil and tension crack is formed at the head of the slope. Subsequent cracks spread from this tension crack towards the toe of the slope. Now the rainwater can easily travel towards the toe of the slope through these cracks. This increases the saturation level at the toe. At the moment when there is too much tension caused due to cracks, the soil fails by sliding.
- The moisture content recordings of sensors along with other properties of soil sample were used to calculate the saturation values at the time of failure. There were a total of three locations for which we obtained the degree of saturation. It was clear from my findings that instrumental changes were most evident along the superficial layer of the slope. The saturation value deep inside the slope in both the models were not that significant but they were present for sure. The toe area manifested the highest level of saturation degree in both the models. This marks the importance of monitoring of toe area through sensors for predicting landslide. Specific thresholds of degree of saturation can be decided for particular slopes and can be incorporated into warning system so that timely warning could be given. It is noteworthy that the initial signs of failure were seen on the top end of the slope and not on toe area, as the first crack appeared on the head of slope. Also, it can be seen from my results that the soil need not to be 100% saturated for it to fail.
- The failure time was found out to be inversely proportional with the steepness of slope, as 70° slope took less time to fail than the 60° slope. This is obvious as greater slope angle leads to more instability therefore leading to faster collapse.

- Another major feature observed from the test results was that, the maximum depth of failure surface was more in 60° slope. It was also seen that for greater depth of failure surface, the extent of slope collapse was larger. So, it can be concluded that with decreasing slope angles, the depth of failure surface decreased and thus the size of landslide increased.

5.2 Future opportunities

There are still possibilities for further exploration. The following points could be considered –

- A different type of soil can be used for making slope models. A more practical approach is to use soil from site of actual landslide and prepare models having same properties as that of actual slope.

- Pore water pressure could be monitored in flume testing. For a particular soil type, the variations of pore water pressure can provide us better insights about the failure process happening in that soil. We can also study the effect of pore water pressure in creating both stability and instability in soil slopes.

- Using a proper rainfall simulator, different intensities of rainfall could be administered on slopes made from same soil. The effects of varying rainfall intensities can be studied. Also the accurateness of results can be improved by using better quality monitoring instruments.

- Model slopes can be tested under dynamic conditions using shaking table.

REFERENCES

1. Oka, H. (1972). Impacts by the "artificial landslide": re-examine the rage of nature. *Kagaku Asahi*, *32*(1), 152-153.
2. Kutara, K., & Ishizuka, H. (1982). Seepage flow in the embankment and stability of slope during rain. *Tsuchi-to-kiso, Paper*, (1330).
3. YAGI, N., YATABE, R., & ENOKI, M. (1985). Laboratory and field experiments on prediction method of occuring time of slope failure due to rainfall. *Landslides*, *22*(2), 1-7_1.
4. Yamaguchi, I., Nishio, K., Kawabe, H., Shibano, H., & Iida, C. (1989). Initiation and fluidization of an artificial landslide: Field experiment in Yui Shizuoka Prefecture, Japan. *Shinrin Kosoku (Areal Survey)*, *158*, 3-9.
5. Iverson, R. M., Reid, M. E., & LaHusen, R. G. (1997). Debris-flow mobilization from landslides. *Annual Review of Earth and Planetary Sciences*, *25*(1), 85-138.
6. Iverson, R. M. (1997). The physics of debris flows. *Reviews of geophysics*, *35*(3), 245-296.
7. Hunger, O., & Morgenstern, N. R. (1984). Experiments on the flow behaviour of granular materials at high velocity in an open channel. *Geotechnique*, *34*(3), 405-413.
8. Eckersley, D. (1990). Instrumented laboratory flowslides. *Geotechnique*, *40*(3), 489-502.
9. DM, C. (1991). A simple definition of a landslide. *Bulletin of the international association of engineering geology*, *43*(1), 27-29.
10. Burns, S. F. (2006). Landslides in Practice: Investigation, Analysis and Remedial/Preventative Options in Soils: (Derek H. Cornforth).
11. Varnes, D. J. (1978). Slope movement types and processes. *Special report*, *176*, 11-33.
12. Cruden, D. M. (1993). Cruden, DM, Varnes, DJ, 1996, Landslide Types and Processes, Transportation Research Board, US National Academy of Sciences, Special Report, 247: 36-75. *Landslides Eng. Pract*, *24*, 20-47.
13. Singh, Ravinder. (2018). Landslide problems and management in Himalaya.
14. Rahardjo, H., Lee, T. T., Leong, E. C., & Rezaur, R. B. (2005). Response of a residual soil slope to rainfall. *Canadian Geotechnical Journal*, *42*(2), 340-351.
15. Ambraseys, N., & Bilham, R. (2000). A note on the Kangra M s= 7.8 earthquake of 4 April 1905. *Current Science*, *79*(1), 45-50.
16. Eckersley, D. (1990). Instrumented laboratory flowslides. *Geotechnique*, *40*(3), 489-502.

17. Tohari, A., Nishigaki, M., & Komatsu, M. (2007). Laboratory rainfall-induced slope failure with moisture content measurement. *Journal of Geotechnical and Geoenvironmental Engineering*, *133*(5), 575-587.
18. Tu, X. B., Kwong, A. K. L., Dai, F. C., Tham, L. G., & Min, H. (2009). Field monitoring of rainfall infiltration in a loess slope and analysis of failure mechanism of rainfall-induced landslides. *Engineering Geology*, *105*(1-2), 134-150.
19. Ching-Chuan, H., Yih-Jang, J., Lih-Kang, H., & Jin-Long, L. (2009). Internal soil moisture and piezometric responses to rainfall-induced shallow slope failures. *Journal of Hydrology*, *370*(1-4), 39-51.
20. Catane, S. G., Zarco, M. A. H., Cordero, C. J. N., Kaimo, R. A. N., & Saturay, R. M. (2011). Laboratory Experiments on Steady State Seepage-Induced Landslides Using Slope Models and Sensors. *Science Diliman*, *23*(1).
21. Wicaksana, Y., Kramadibrata, S., & Wattimena, R. K. (2014, October). A Laboratory Scale of Physical Modeling of Slope Failure Generated by Centrifugal Acceleration with Several Water Content Scenarios. In *ISRM International Symposium-8th Asian Rock Mechanics Symposium*. OnePetro.
22. Bucky, P. B. (1931). *Use of models for the study of mining problems* (No. 44). American Institute of Mining and Metallurgical Engineers, Incorporated.
23. Wu, L. Z., Huang, R. Q., Xu, Q., Zhang, L. M., & Li, H. L. (2015). Analysis of physical testing of rainfall-induced soil slope failures. *Environmental earth sciences*, *73*, 8519-8531.
24. Chueasamat, A., Hori, T., Saito, H., Sato, T., & Kohgo, Y. (2018). Experimental tests of slope failure due to rainfalls using 1g physical slope models. *Soils and Foundations*, *58*(2), 290-305.
25. Zhang, S., Zhang, X., Pei, X., Wang, S., Huang, R., Xu, Q., & Wang, Z. (2019). Model test study on the hydrological mechanisms and early warning thresholds for loess fill slope failure induced by rainfall. *Engineering Geology*, *258*, 105135.
26. Paswan, A. P., & Shrivastava, A. K. (2022). Modelling of rainfall-induced landslide: a threshold-based approach. *Arabian Journal of Geosciences*, *15*(8), 795.
27. Eller, H., & Denoth, A. (1996). A capacitive soil moisture sensor. *Journal of Hydrology*, *185*(1-4), 137-146.
28. Kurniawan, A. (2019). *Internet of Things Projects with ESP32: Build exciting and powerful IoT projects using the all-new Espressif ESP32*.

29. Maureira, M. A. G., Oldenhof, D., & Teernstra, L. (2011). ThingSpeak–an API and Web Service for the Internet of Things. *World Wide Web*, *25*, 1-4..
30. Chen, Z. Y., & Shao, C. M. (1988). Evaluation of minimum factor of safety in slope stability analysis. *Canadian geotechnical journal*, *25*(4), 735-748.